LETTER

Compressed Sensing EEG Measurement Technique with Normally Distributed Sampling Series

Yuki OKABE[†], *Nonmember*, **Daisuke KANEMOTO**[†a)], *Member*, **Osamu MAIDA**[†], *Nonmember*, *and* **Tetsuya HIROSE**[†], *Member*

SUMMARY We propose a sampling method that incorporates a normally distributed sampling series for EEG measurements using compressed sensing. We confirmed that the ADC sampling count and amount of wirelessly transmitted data can be reduced by 11% while maintaining a reconstruction accuracy similar to that of the conventional method.

key words: *EEG, low-power consumption, compressed sensing, random undersampling, normal distribution*

1. Introduction

In recent years, electroencephalogram (EEG) measurements have been actively studied in the medical and engineering fields because they can be used for the early detection of brain diseases such as Alzheimer's disease and for confirmation of health status [1]. In conventional EEG measurements, the measurement device is attached directly to the head of the subject by a cable, and the restraint caused by prolonged measurement causes a burden and discomfort to the subject. In recent years, wireless EEG measurement devices have attracted considerable attention because they cause less discomfort to the subject [2]. However, wireless EEG measurement devices are battery-powered. A low-power consumption technique should be incorporated in the circuit design to realize a lightweight device with a small battery and long-term measurement capabilities.

In the general flow of wireless EEG measurements, the sensing unit acquires EEG signals from the head of the subject. Because the magnitude of the acquired EEG signal is weak, it is amplified through an analog circuit [3]. Next, the analog-to-digital converter (ADC) converts the analog EEG signal into a digital signal, which is then sent to the data processing unit for analysis. It has been reported that approximately 70% of the total system power is consumed when the signal is transmitted by this radio [4]. Therefore, we have been studying EEG measurement frameworks using compressed sensing (CS) [5] to reduce the power consumption during wireless transmission [6]–[9].

Among CS approaches, random undersampling has received considerable attention for simplifying the ADC implementation. One of the random undersampling methods uses a continuous uniform distribution as a pseudorandom distribution with a certain interval sampling width. This approach can reduce the ADC power consumption [10]. However, an optimal distribution of the sampling series has not been proposed to further reduce the ADC power consumption, and it is thought that the distribution of the sampling series needs to be improved to achieve further reduction in ADC and wireless transmission power consumption.

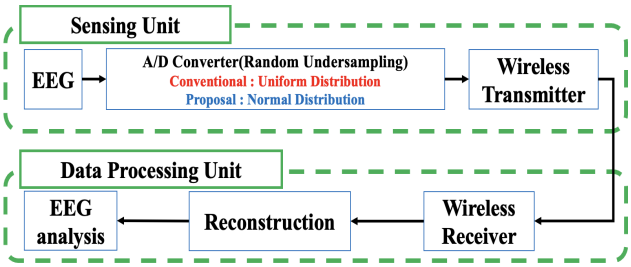

Fig. 1 EEG mesurement framework.

We propose an ADC sampling scheme that achieves low power consumption during wireless transmission in the EEG measurement framework (Fig. 1) using random undersampling. To focus on the discussion pertaining to sampling, the EEG measurement framework without independent component analysis (ICA) was considered in this letter.

The remainder of this letter is organized as follows. Section 2 describes the background of the study. Section 3 explains the details of the proposed sampling scheme. In Sect. 4, we describe the condition settings and results of the simulation using the proposed sampling scheme. Finally, we conclude the paper in Sect. 5.

2. Research Background

2.1 Compressed Sensing Theory

CS theory is a method used to reconstruct a signal from a smaller number of observations than the number of samples originally required. In particular, CS is used to solve the problem of finding $\mathbf{x}$ of size N, which can be shown as a k-sparse signal in a certain basis matrix Ψ. The term "k-sparse" means that the number of nonzero elements in the vector $\mathbf{s}$, denoted by $\mathbf{x}=\Psi\mathbf{s}$, is k pieces. Using CS to multiply the input signal $\mathbf{x}$ by the $M \times N$ observation matrix Φ, we

Manuscript received November 8, 2021.
Manuscript revised March 3, 2022.
Manuscript publicized April 22, 2022.

[†]The authors are with the School of Engineering, Division of Electronic and Information Engineering, Osaka University, Suita-shi, 565-0871 Japan.
a) E-mail: dkanemoto@eei.eng.osaka-u.ac.jp (Corresponding author)

DOI: 10.1587/transfun.2021EAL2099

obtain the compressed (observed) signal **y**. Therefore, the compressed signal **y** of size M can be written as

$$\mathbf{y} = \Phi\mathbf{x} = \Phi\Psi\mathbf{s} = \mathbf{A}\mathbf{s}. \quad (1)$$

$\mathbf{A}=\Phi\Psi$, and **A** is called the sensing matrix. When the signal is compressed, the dimension of **y** becomes much lower than the dimension of **s**, resulting in a problem that is difficult to solve with no uniquely determined solution. However, if the vector **s** is sparse and has many zero elements, it can be reconstructed by solving the following equation:

$$\min||\mathbf{s}||_0 \text{ subject to } \mathbf{y} = \mathbf{A}\mathbf{s}. \quad (2)$$

The l_0 minimization problem is known to be NP-hard, which makes it difficult to implement in applications. The so-called greedy algorithm is a powerful method for solving this problem efficiently. In this study, we simulated the reconstruction by using block sparse Bayesian learning [11], which is a greedy algorithm that shows excellent results in EEG reconstruction [12].

2.2 Conventional Approach to Sampling Interval

When implementing a CS system using random undersampling, the sampling frequency of the ADC is not fixed; therefore, the sampling period of the narrowest sampling interval becomes the maximum ADC sampling frequency. To reduce the ADC power consumption, the maximum sampling frequency should be reduced. The sampling period of the narrowest sampling interval must be increased to reduce the maximum sampling frequency. During the sampling of a continuous uniform distribution with a widened sampling interval defined in the conventional method, with a compression factor of N/M, the sampling interval should be taken within the range of N/M and $2(N/M)$-1 [10].

In Fig. 2, when the sampling interval time between the nearest neighboring samples is Δt and the sampling interval at this time is defined as 0, a sampling interval time of $((N/M)+1)\Delta t$ or more is always implemented; therefore, the maximum sampling frequency $fs_{interval}$ is as follows:

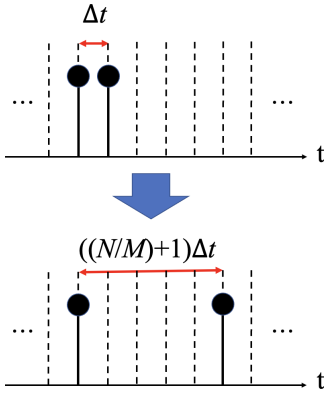

Fig. 2 Concept of the sampling interval of the nearest neighboring samples for ADC.

$$fs_{interval} = \frac{1}{((N/M)+1)\Delta t}. \quad (3)$$

From Eq. (3), by increasing the sampling period of the narrowest sampling interval, the maximum sampling frequency can be decreased, thus reducing the ADC power consumption.

3. Proposed Sampling Method

Section 2.2 covers the importance of widening the sampling interval to reduce the ADC power consumption. In this section, we discuss the distribution of the sampled series within the sampling interval width.

In CS, a smaller M value reduces the number of data points to be handled, which reduces power consumption during wireless transmission, which consumes the most power. We propose an ADC sampling scheme that minimizes the M value. In the conventional sampling series with a continuous uniform distribution, as shown in Fig. 3, even if the random pattern is changed, the probability density of each pattern is constant, and therefore a significant decrease in M cannot be expected. Therefore, we reduce the number of samples at the narrowest sampling interval, denoted by N/M. This approach reduces the number of samples to be taken, thus decreasing the M values.

For example, reducing the number of samples in the narrowest sampling interval, requires an increase in the number of samples in the sampling interval of $2(N/M)$-1. To increase the number of samples in $2(N/M)$-1, we adopt the normal distribution with $2(N/M)$-1 as the mean value (Fig. 3). In the case of the sampling series using the normal distribution, as the number of sampling frequencies of $2(N/M)$-1 is increased, the value of M is decreases more. Thus, lower power consumption can be expected, because the amount of wirelessly transmitted data can be reduced.

The graph of a general normal distribution is symmetrical with mean μ at the center, and as the variance (the standard deviation σ) is reduced, the peak of the mean value

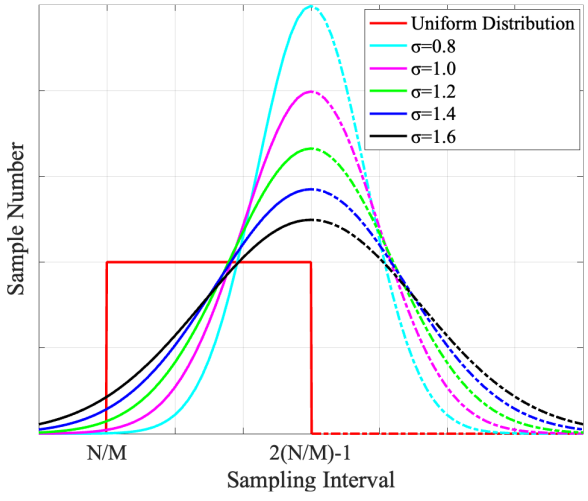

Fig. 3 Comparison of distribution.

becomes higher and sharper, thus reducing the number of M values. In contrast, when σ is increased, the peak of the mean value is lower and spreads to the left and right. Thus, the number of samples in the narrowest sampling interval of N/M increases, as does the number of M values. Therefore, by changing σ, one of the variables constituting the normal distribution, we implement a sampling method with low power consumption and no effect on the reconstruction accuracy. Fig. 3 shows an example for $\sigma = 0.8$ to 1.6. In addition, the sampling series used is the left half of the distribution shown in Fig. 3, and the right half shown by the dotted line is not used.

4. Design and Evaluation

4.1 Implementation Conditions

When implementing a multichannel signal system (such as the EEG signal used herein) in a single ADC, a multiplexer (MUX seen in Fig. 4) is generally used. In this simulation, a four-channel MUX was used. As shown in Fig. 4, a block was set up for each of the four sample points, and the order of the selected channels was determined by a random number within each block. For example, the order of channels to be selected in the first block in Fig. 4 is Ch 3, Ch 4, Ch 1, Ch 2. In addition, the sampling interval of the ADC was designed to be $5\Delta t$ to $8\Delta t$. The proposed method uses a normal distribution biased toward the maximum sampling interval of $8\Delta t$, whereas the conventional method uses a continuous uniform distribution for the frequency distribution that determines the ADC sampling interval. As shown in Fig. 4(a), (b), the number of samples acquired by the proposed method is smaller than that by the conventional method within the same time interval, resulting in a design that reduces the amount of data transmitted during wireless transmission.

Because the maximum sampling interval of $8\Delta t$ is 7 when Δt is set as the sampling interval 0, we set $\mu = 7$ as the mean of the normal distribution. This sampling series was implemented in MATLAB. This study used the EEG waveform measured during eye opening of a healthy male in his 20s, sampled at 1000 Hz from 16 electrodes arranged according to the 10-20 Electrode Positioning System [13] with 3 s per frame (3000 samples). The normalized mean square error (NMSE) was used as an evaluation index for the accuracy of EEG waveform reconstruction. Assuming that the original signal is $\mathbf{x}$ and the reconstructed signal is $\hat{\mathbf{x}}$, the NMSE can be expressed as

$$\mathrm{NMSE} = \frac{||\hat{\mathbf{x}} - \mathbf{x}||_2^2}{||\mathbf{x}||_2^2}. \tag{4}$$

As the original and reconstructed signals become closer to equal, the value of the numerator becomes closer to zero; therefore, an NMSE value closer to zero indicates better reconstruction accuracy. The NMSE values calculated in this study were the 150-frame averages of the EEG.

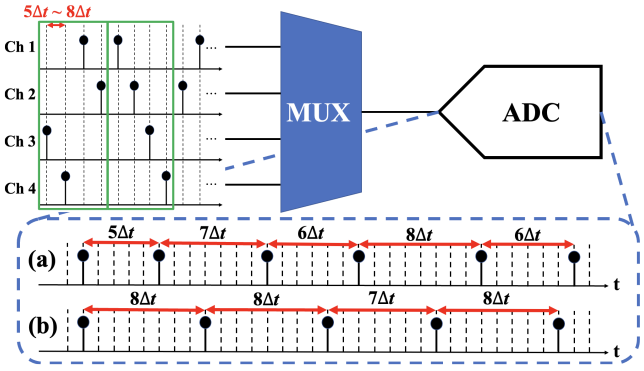

Fig. 4 ADC mechanism using a MUX. (a) Conventional [10]. (b) Proposal.

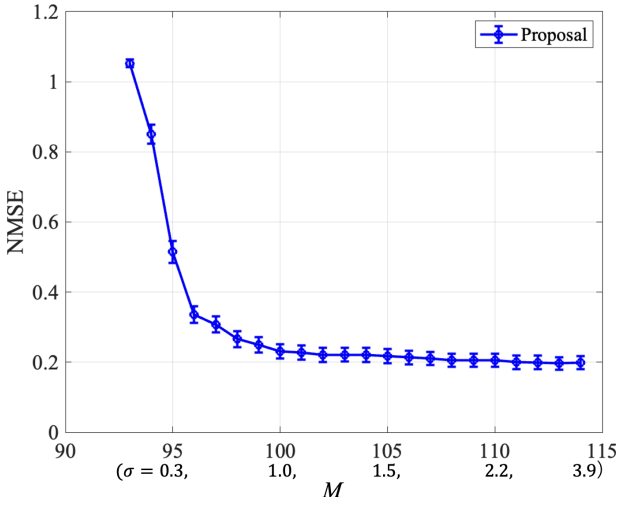

Fig. 5 Reconstruction accuracy with change in standard deviation.

4.2 Results

The following results were obtained for the electrode configuration FP1 of the 10-20 Electrode Positioning System [13], which corresponded to Ch 1 in this study. The simulation results for the standard deviation $\sigma = 0.1$ to 3.9 of the normal distribution are shown in Fig. 5. σ and M are related, as explained in Sect. 3; for example, $\sigma = 0.3$ corresponds to $M = 95$ (Fig. 5). The error bars in the graph represent the standard error. The standard error is a measure of the degree to which the sample mean varies with respect to the population mean when the sample mean is calculated from a sample drawn from the population. In this study, the error bars are shown for a population of 100 random seed numbers.

Figure 5 shows that when M is significantly low, the reconstruction accuracy is also low. Also, the sampling interval of the ADC in this study, $5\Delta t$ to $8\Delta t$, cannot be achieved when $\sigma = 0.8$ or less. Therefore, it is necessary to discuss the accuracy of the reconstruction for $\sigma = 0.9$ and above. Figure 6 shows the enlarged result of displaying the values from $\sigma = 0.9$ to 3.9 in Fig. 5. In Fig. 6, compares the reconstruction accuracy and the amount of wirelessly transmitted

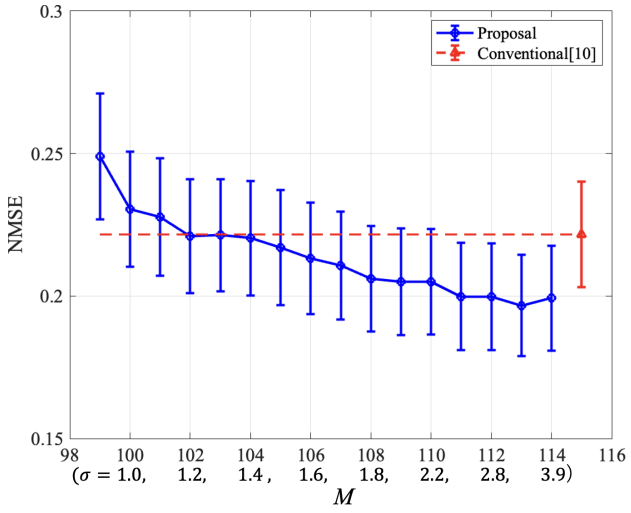

Fig. 6 Comparison of reconstruction accuracy with conventional methods.

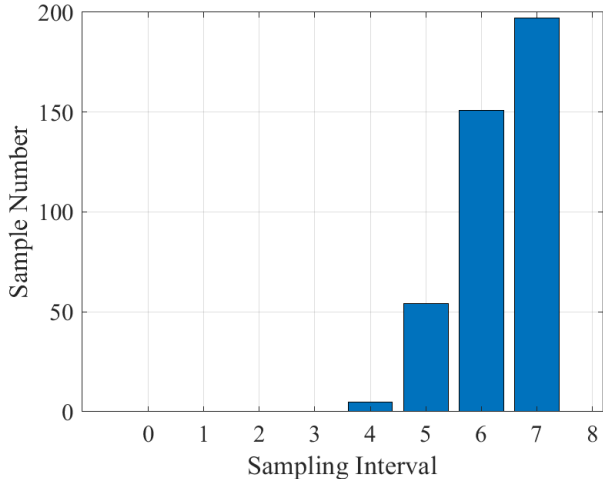

Fig. 7 Proposed sampling series example ($\sigma = 1.2$, $M = 102$).

information as the uniform distribution of the conventional method and the normal distribution of the proposed method. Figure 6 shows that the reconstruction accuracy at $M = 102$ ($\sigma = 1.2$) is the almost same as that of the conventional method ($M = 115$ [10]). An example of the sampling series of the four-channel MUX created in this simulation is shown in Fig. 7. It can be seen that the distribution of sampling intervals follows a normal distribution, rather than a conventional uniform distribution. The proposed sampling scheme of the ADC can reduce the amount of transmitted information in wireless transmission by 11% owing to the decrease in the number of ADC samples.

Finally, the energy efficiency of the ADC with the proposed sampling series is compared with the conventional one [10]. In designing an ADC circuit, the number of samples as well as $fs_{interval}$ often affects the power consumption. Figure of Merit (FoM) [14] is widely used as an indicator of power efficiency of ADCs by utilizing power consumption, number of effective bits, and sampling frequency. In general, the sampling frequency of ADCs is often fixed. Since the sampling frequency is variable in random undersampling, FoM was calculated using the average of the frequency $fs_{average}$ as well as [10].

Table 1 Comparison of energy efficiency using FoM.

	FoM [fJ/conv]
Nyquist sampling [10]	92
Conventional (Uniform Distribution) [10]	12.2
Proposal (Normal Distribution)*	10.8

* The FoM of the proposed method is estimated for the same ADC based on in [10].

$$\text{FoM} = \frac{P}{2^{\text{ENOB}} fs_{average}}. \tag{5}$$

Here, P is the power consumption of ADC, and ENOB indicates the number of effective bits. Since the conventional method adopts uniform distribution and the proposed method adopts normal distribution, the average sampling interval is higher and the average sampling frequency is lower in the proposed method. Therefore, $fs_{average}$ of the proposed method is 0.88 times smaller than that of the uniform distribution. Next, the above results were applied to the ADC reported in the previous study [10]. The FoM estimation results are shown in Table 1. Given that the value of FoM is determined when ADC is selected, a reduction in sampling frequency implies a reduction in $P/2^{\text{ENOB}}$. The Nyquist sampling indicates the FoM when the prototype ADC in [10] is operated at the Nyquist rate. Conventional FoM is the measured FoM of the ADC when utilizing compressed sensing with uniform distribution as discussed in [10]. If the proposed sampling series utilizes normal distribution, the estimated FoM can be reduced to 11% when calculated using Eq. (5) because the average frequency is suppressed.

5. Conclusions

In this letter, we propose a sampling scheme using random undersampling for multi-channel signals, such as EEG signals. The sampling series of conventional ADCs uses a continuous uniform distribution; however, for low power consumption during wireless transmission, we adopt a sampling series by incorporating a normal distribution. We proposed a sampling scheme that can reduce the amount of data during wireless transmission by adjusting σ of a normal distribution, and we discussed the relationship between M and NMSE. We could reduce the amount of information transmitted during wireless transmission by 11% while maintaining a reconstruction accuracy similar to that of the conventional sampling scheme. By designing a suitable distribution for the sampling series of the ADC, we could reduce the power consumption of the ADC and wireless transmission.

Acknowledgments

This work was supported by JSPS KAKENHI Grant Number

JP21H03410. This work was supported by JKA and its promotion funds from AUTO RACE.

References

[1] Y. Kang, J. Escudero, D. Shin, E. Ifeachor, and V. Marmarelis, "Principal dynamic mode analysis of EEG data for assisting the diagnosis of Alzheimer's disease," IEEE J. Transl. Eng. Health Med., vol.3, Feb. 2015.

[2] S. Consul-Pacareu, R. Mahajan, M.J. Abu-Saude, and B.I. Morshed, "NeuroMonitor: A low-power, wireless, wearable EEG device with DRL-less AFE," IET Circuits, Devices & Systems, vol.11, no.5, pp.471–477, May 2017.

[3] J. Xu, R.F. Yazicioglu, P. Harpe, K.A.A. Makinwa, and C.V. Hoof, "A 160 μW 8-channel active electrode system for EEG monitoring," Proc. 2011 IEEE International Solid-State Circuits Conference, pp.20–24, Feb. 2011.

[4] R.F. Yazicioglu, S. Kim, T. Torfs, H. Kim, and C.V. Hoof, "A 30 μW analog signal processor ASIC for portable biopotential signal monitoring," IEEE J. Solid-State Circuits, vol.46, no.1, pp.209–223, Jan. 2011.

[5] D. Donoho, "Compressed sensing," IEEE Trans. Inf. Theory, vol.52, no.4, pp.1289–1306, April 2006.

[6] D. Kanemoto, S. Katsumata, M. Aihara, and M. Ohki, "Framework of applying independent component analysis after compressed sensing for electroencephalogram signals," Proc. 2018 IEEE Biomedical Circuits and Systems Conference (BioCAS), pp.17–19, Oct. 2018.

[7] S. Katsumata, D. Kanemoto, and M. Ohki, "Applying outlier and independent component analysis for compressed sensing EEG measurement framework," Proc. 2019 IEEE Biomedical Circuits and Systems Coference (BioCAS), pp.1–4, Oct. 2019.

[8] D. Kanemoto, S. Katsumata, M. Aihara, and M. Ohki, "Compressed sensing framework applying independent component analysis after undersampling for reconstructing electroencephalogram signals," IEICE Trans. Fundamentals, vol.E103-A, no.12, pp.1647–1654, Dec. 2020.

[9] K. Nagai, D. Kanemoto, and M. Ohki, "Applying K-SVD dictionary learning for EEG compressed sensing framework with outlier detection and independent component analysis," IEICE Trans. Fundamentals, vol.E104-A, no.9, pp.1375–1378, Sept. 2021.

[10] M. Trakimas, R.J. D'Angelo, S. Aeron, T. Hancock, and S. Sonkusale, "A compressed sensing analog-to-information converter with edge-triggered SAR ADC core," IEEE Trans. Circuits Syst. I, Reg. Papers, vol.60, no.5, pp.1135–1148, May 2013.

[11] Z. Zhang and B.D. Rao, "Recovery of block sparse signals using the framework of block sparse Bayesian learning," Proc. 2012 IEEE International Conference on Acoustics, Speech and Signal Processing (ICASSP), Kyoto (Japan), pp.3345–3348, March 2012.

[12] Z. Zhang, T.P. Jung, S. Makeig, and B.D. Rao, "Compressed sensing of EEG for wireless telemonitoring with low energy consumption and inexpensive hardware," IEEE Trans. Biomed. Eng., vol.60, no.1, pp.221–224, Jan. 2013.

[13] F. Sharbrough, G. Chatrian, H.L. RP Lesser, M. Nuwer, and T. Piction, "American electroencephalographic society guidelines for standard electrode position nomenclature," J. Clin. Neurophysiol, vol.8, no.2, pp.200–202, 1991.

[14] R.H. Walden, "Analog-to-digital converter survey and analysis," IEEE J. Sel. Areas Commun., vol.17, no.4, pp.539–550, April 1999.